Chemistry Research Journal, 2020, 5(5):16-30

Available online www.chemrj.org

Research Article

ISSN: 2455-8990
CODEN(USA): CRJHA5

Molecular docking, molecular dynamics simulations and ADME study to identify inhibitors of Crimean-Congo Hemorrhagic Fever (CCHF) viral ovarian tumor domain protease (vOTU)

Emmanuel Israel Edache[1,2]*, Adamu Uzairu[2], Paul Andrew Mamza[2], Gideon Adamu Shallangwa[2]

[1]Department of Pure and Applied Chemistry, University of Maiduguri, Brono State, Nigeria
[2]Department of Chemistry, Ahmadu Bello University, Zaria, Nigeria
Email: edacheson2004@gmail.com, Phone number: +2348066776802

Abstract In this study, we used molecular docking, molecular dynamics (MD) simulation and ADME studies to analyze the interactions of a series of derivatives as potent inhibitors of Crimean-Congo Hemorrhagic Fever (CCHF) viral ovarian tumor domain protease (vOTU). Docking studies predict the binding mode and the interactions between the ligand and the protein. Molecular dynamics simulations results reveal that the complex of the ligand and the receptor protein is stable at 310K. For the prediction of blood-brain barrier penetration the PowerMV software was able to predict the BBB profile for most of the drugs. Lipinski's and Veber's parameters, Ligand efficiency (LE), Lipophilic Efficiency (LipE), are described and discussed, to understand the biological activity of the compounds. All the results can provide more profitable information for our further drug design.

Keywords Crimean-Congo hemorrhagic fever (CCHF), Molecular Docking, Molecular dynamics simulation, ADME

1. Introduction

Crimean-Congo hemorrhagic fever (CCHF) is a well-known tick-borne viral disease that can affect human beings [1, 2]. It is a member of the Bunyaviridae family of RNA viruses [2-4]. CCHF virus is among several tick-transmitted viruses that have gathered increasing interest due to their emergence in Europe [3, 5], which is at least partially blamed on global climate change. Clinical disease is rare in infected mammals, but it is commonly severe in infected humans [6]. Occurrences of illness are usually attributable to handling infected animals or people. Humans affected by Crimean-Congo hemorrhagic fever (CCHF) is characterized by high fever, prostration, and severe hemorrhage [3, 7]. Additionally, infection with CCHF and the closely related Dugbe virus (DUGV), Hazara (HAZV), Nairobi sheep disease virus (NSDV), and Ganjam virus (GANV) in sheep negatively impacts local economies through high livestock mortality and limiting of trade with the affected areas [3, 4, 8]. There is no FDA approved vaccine or treatment for CCHFV, which is considered one of the most dangerous emerging human pathogens as well as representing a significant bioterrorist threat agent [7]. X-ray crystal structures have been solved of CCHFV vOTU alone [8], in complex with Ub, [6, 9], and in complex with ISG15 [8, 9], which revealed a conserved OTU-like fold of its eukaryotic counterparts. Investigators have identified an ovarian tumor domain protease (OTU) located in the L-protein of CCHFV and revealed its potential role in suppressing the innate immune

response [3, 10, 11]. This cysteine protease signifies a new viral taxonomic group of OTU domain proteases (vOTUs), which have also been located in economically devastating viruses such as porcine reproductive respiratory syndrome virus (PRRSV) and rice stripe virus (RSV) [6, 7]. Mostly, OTUs have been linked to ubiquitin (Ub) removal and/or remodeling of Ub-conjugated proteins [12], also known as deubiquitination, placing them among five protease super-families that facilitate signal transduction cascades and play key roles in protein stability [3, 11, 13]. vOTU molecular analysis would allow an assessment of whether the molecular analysis scaffold can serve as a basis to selectively inhibit other viral and eukaryotic ovarian tumor domain proteases, as well as potentially leading to the development of prophylactics targeting vOTUs and their eukaryotic superfamily relatives that negatively regulate the human innate response [2-4, 11].

The primary objective of pharmaceutical chemistry and medicinal chemistry is the design and discovery of new compounds that are suitable for use as drugs. This practice involves a group of workers from a wide range of disciplines such as chemistry, biology, biochemistry, pharmacology, mathematics, medicine, and computer science, amongst others. Drug finding may also require essential research into the biological and chemical nature of the diseased state. These and other aspects of drug design and discovery needcontribution from specialists in many other fields and so medicinal chemists and pharmacists need to have framework knowledge of the relevant aspects of these fields. Molecular docking, absorption, distribution, metabolism and excretion (ADME) and Molecular Dynamics (MD) simulation studies are generally performed to obtain the stable structure of a protein concerning time, temperature, kinetic energy and potential energy and how a ligand is interacting with its biological target [14], as a drug in the human body and to support the conclusions of *in vivo, in vitro* studies and discovery of new inhibitors against the target on this pathway might be helpful for the treatment of Crimean-Congo hemorrhagic fever (CCHF).

2. Materials and Methods

In this work, DFT [15] has been employed in the form of Becke`s three-parameter hybrid exchange functional [16] (B3LYP) with Lee-Yang-Parr correlation functional [17]. The standard split-valence basis set added with diffuse as well as polarization functions 6-311+G (d, p) is used throughout these calculations. The Spartan'14 version 1.1.4 program [www.wavefun.com] is used to perform all the DFT computations. The data set used in this study was taken from PubChem [PubChem AID: 720577; https://pubchem.ncbi.nlm.nih.gov/bioassay/720577] and is shown in Table 1. This set contains the values of the inhibitors of Crimean-Congo Hemorrhagic Fever (CCHF) viral ovarian tumor domain protease (vOTU): Pep-AMC substrate". The 3D structure of Domain of Crimean Congo Hemorrhagic Fever Virus in complex with Ubiquitin was obtained from PDB (PDB ID: 3PHW) [18] accessed at the URL (http://www.rscb.org/pdb). The water molecules and all other heteroatoms were removed from the protein crystal structure as shown in Figure 1a. In this study, docking of 62 derivatives against 3PHW has performed using Molegro Virtual Docker v6.0.1 [19] and PyRx software v0.8. Also, the electrostatic potentials of the ligand-binding site for 3phw were calculated by the electrostatic protocol that has been incorporated into Discovery Studio visualizer v16.1.0.15350.

Table 1: Compounds PUBCHEM_CID and observed pIC_{50}

Compd	PUBCHEM_CID	pIC_{50}	Compd	PUBCHEM_CID	pIC_{50}
1	713096	5.822	32	24761366	5.322
2	774975	5.202	33	22829045	5.874
3	272514	5.884	34	9609431	5.343
4	1405137	5.2	35	5824722	5.701
5	11834470	5.982	36	6023694	5.907
6	8143087	5.084	37	5824727	5.601
7	2044030	5.119	38	6023693	6.271
8	753169	5.161	39	5824726	5.627
9	6032979	5.747	40	6763	5.426
10	4653365	5.265	41	664517	5.284

11	2339359	5.972	42	262093	5.134
12	1736294	6.179	43	6603104	5.338
13	2407446	5.059	44	237102	5.969
14	3095208	5.132	45	11834461	5.625
15	610612	5.111	46	3342467	5.018
16	906542	5.937	47	44602155	5.264
17	286873	5.394	48	15945189	5.377
18	2846928	5.151	49	224618	5.224
19	2133777	5.666	50	2545001	5.114
20	5998602	5.987	51	1910302	5.292
21	9701594	5.742	52	248894	5.004
22	2939678	5.119	53	8816	5.073
23	934233	5.177	54	377877	5.241
24	224810	5.157	55	3711067	6.069
25	5358773	5.336	56	266923	5.96
26	18834	5.589	57	280616	5.302
27	16727377	5.865	58	406008	5.826
28	16727376	5.84	59	14710	5.479
29	2974206	5.947	60	377971	5.287
30	24747653	5.192	61	378196	5.029
31	1475552	5.875	62	392758	5.363

2.1. Molecular Dynamics Simulation of 3PHW

The initial structure of the enzyme (PDB entry code 3phw) [18] was extracted from the Brookhaven Protein Database (PDB http://www.rcsb.org/pdb). The crystal structure of 3phw consisted of four similar chains with inhibitor bound at the binding site. The water molecules and inhibitor were removed and chain A was considered for the MD simulations and docking purpose (Fig. 1).

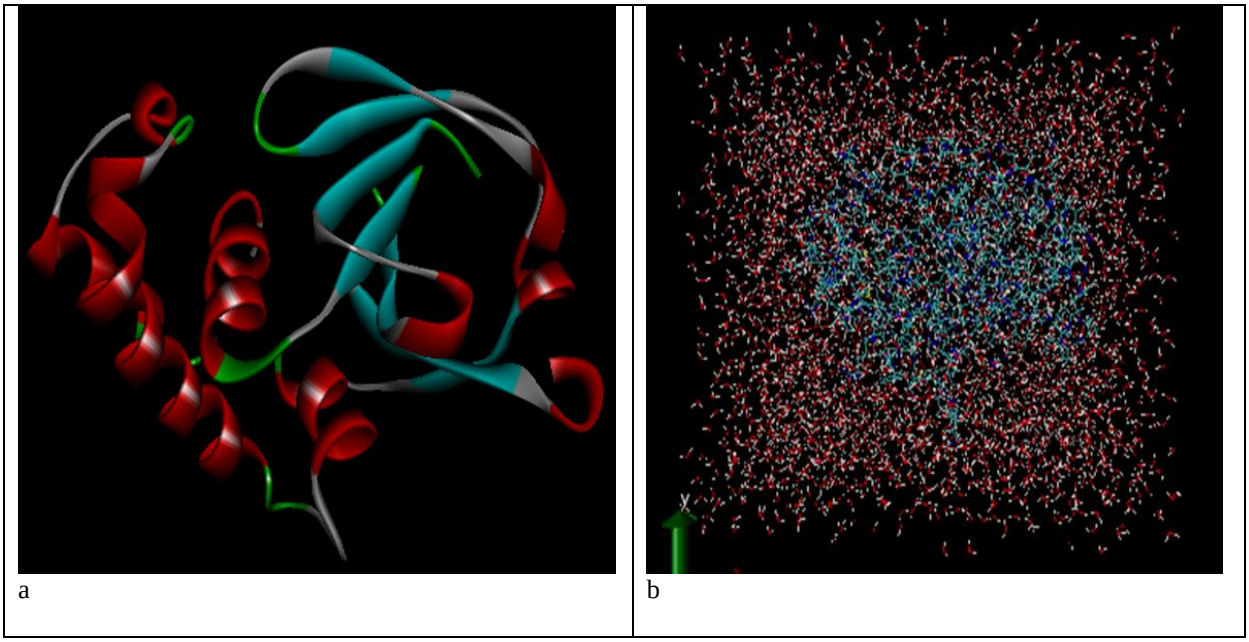

a b

Figure 1: Structure of 3phw chain A [18]; (b) Solvate protein

The MD simulations were performed using the NAMD 2.13 package [20]. The interaction parameters were computed using the CHARMM27 force field (par_all27_prot_lipid.inp). The periodic boundary condition was used and the system was immersed in a cubic water box of extended simple point charge water molecules as shown in figure 2a to calculate the solvated protein. Minimization was performed to optimize the initial structure of the protein-ligand complex. After that, the temperature of the system was gradually heated up from 0K to 310 K in 100ps. Finally, the system was equilibrated at 310 K for 100ps with the NVT ensemble. The MD simulation and results from the analysis were performed on the DELL INSPIRON; Pentium® Dual-Core CPU T4500 @ 2.30GHz and 3GB of RAM, 64-bit-Operating System, x64-based processor.

3. Results and Discussions

Structure of Pep-AMC substrate" (AID 720577), using Ubiquitin AMC as a substrate receptor was involving transferase receptor classification in complex with native ligand (3phw) which gives information about the location, composition and functional conformation opportunity of receptor binding space. In this study, we used the X-ray structure of the OTU Domain of Crimean Congo Hemorrhagic Fever Virus in complex with Ubiquitin ligand (PDB code 3phw) in docking. MVD mechanically finds potential binding sites (also referred to as cavities or active sites) by using its cavity detection procedure [19]. Docking simulations on the enzyme using the same grid coordinates with a re-docking grid box that was placed in the middle position of the ligand, which was at position -6.18, -41.84, -21.15(x, y, z) in Cartesian coordinates. The cavities within a 19.968Å; the surface is 80.64 and a radius of 15Å centered at the experimentally known ligand position were used. The cavities (or binding site) that are acknowledged by the cavity detection algorithm are then used by the guided differential evolution search algorithm to focus the search, to that specific area during the docking simulation. In the case of the crystal structures for 3phw complexes, the program generally identified one binding site (Fig. 2).

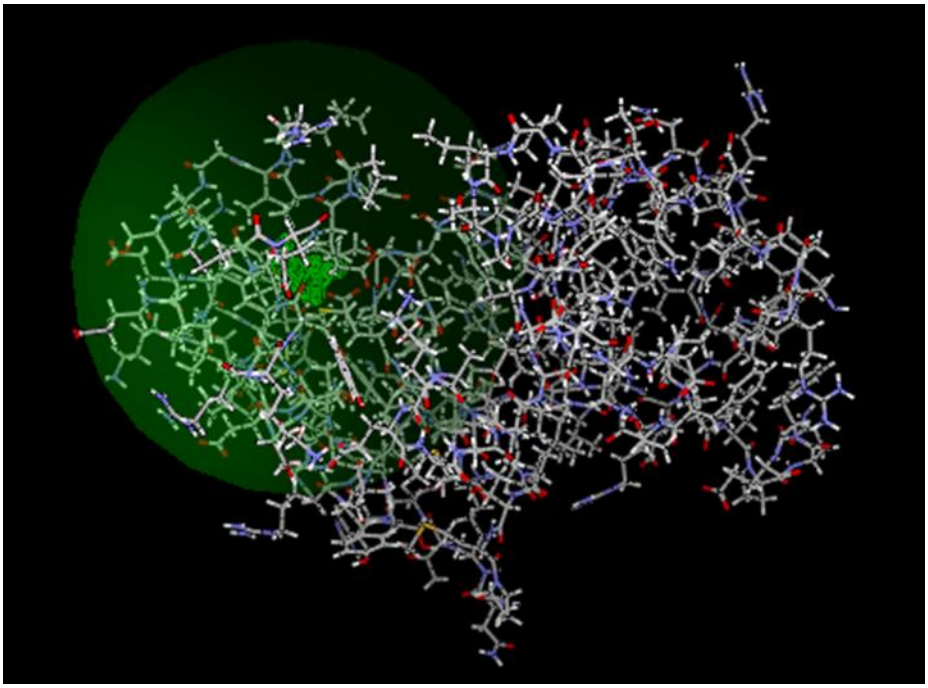

Figure 2: MVD-detected cavity in 3phw; detected cavity green, carbon atoms grey, oxygen atoms red, nitrogen atoms blue

Validation of docking was used to confirm orientation and location of ligand binding that was obtained from docking studies by MVD program with ten replication of each running. And then the parameters must be validated in the crystal structure of the receptor (PDB code 3phw). In each docking run, the best poses were selected based on their MVD re-rank scores, and the re-rank scores were then computed as the final score for each compound. The

MVD score and the re-rank scores of the best poses for each of the docking studies of the ligand with 3phw are summarized in Table 2.

Table 2: Values obtained from the Molegro Virtual Docker

Ligand: Pubchem_CID	Compound number	MolDock Score	Rerank Score	H-Bond
2044030	7	-126.167	-90.1118	-2.86179
2133777	19	-126.7	-79.9667	-4.28752
5998602	20	-126.312	-98.4432	-2.5
5824722	35	-130.306	-97.6302	-5.27059
5824727	37	-131.181	-61.2495	0
5824726	39	-125.404	-101.284	-5.44733
664517	41	-124.699	-67.6781	-1.9009
392758	62	-129.032	-90.8345	-3.12108

The obtained score is between -61.2495 and -101.284 kcal/mol. The best docking poses obtained based on the MVD re-rank score for modified compounds of the crystal structures of 3phw are presented in Figure 3. Docking studies of ligands with 3phw showed the presence of hydrogen bonding between these compounds with the proteins of 3phw. It is revealed that the COOH group of compound 39 has hydrogen bond interaction with Arg92 and Val82. The docking results compound 39 with 3phw reveals no electrostatic interactions but it has a hydrogen bonding and steric interaction between the ligand to receptor (Fig. 3). The COOH group of compound 20 has hydrogen bond interaction with Leu81 with 3phw. The aromatic group and NH group of these compounds have steric interaction with Arg92, Val82, Ser101, Leu103, and Met93 from 3phw (Fig. 3).

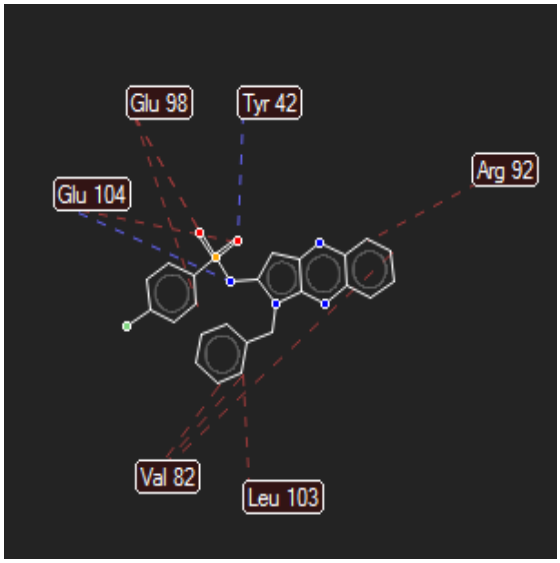

Compound 7

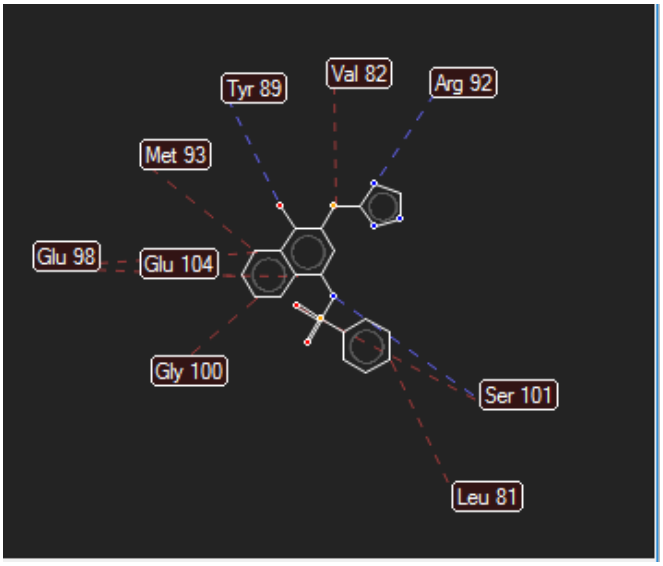

Compound 19

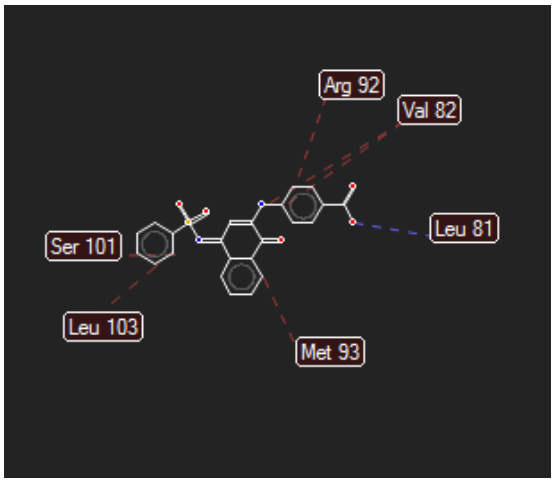

Compound 20

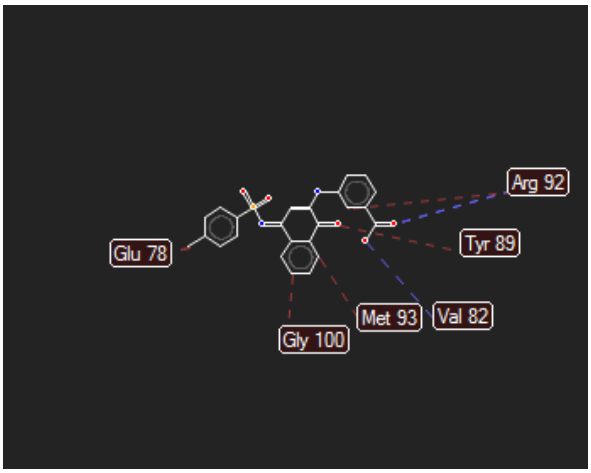

Compound 35

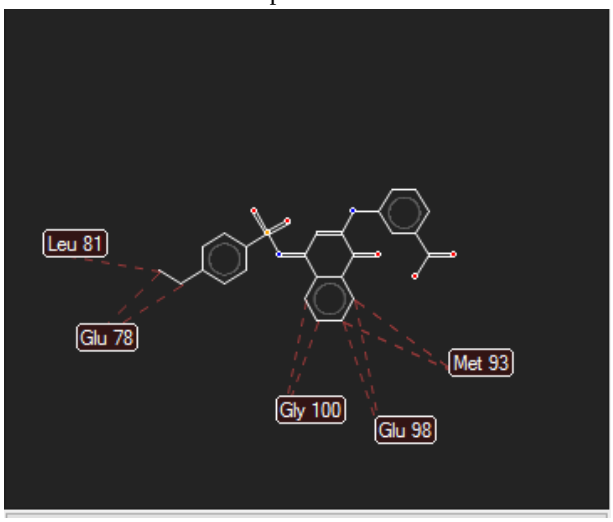

Compound 37

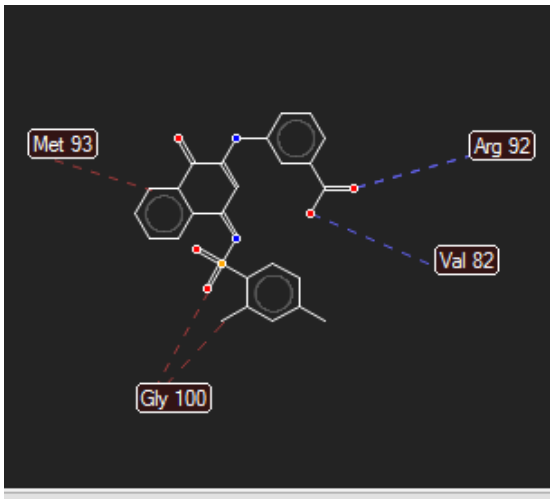

Compound 39

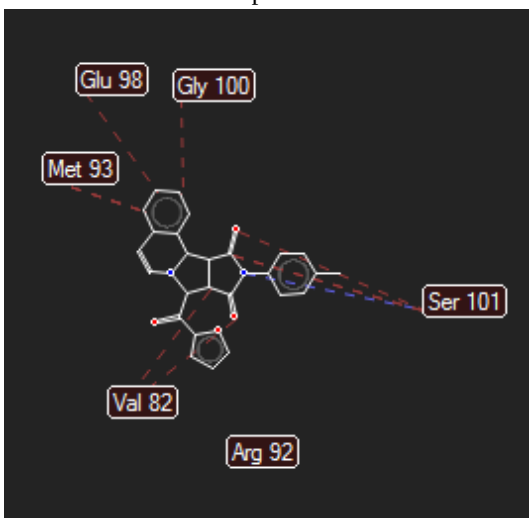

Compound 41

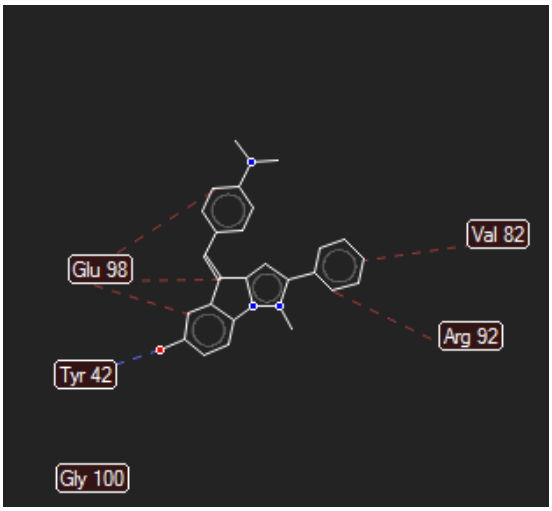

Compound 62

Figure 3: Hydrogen bond (blues lines) and steric interaction (red lines) of ligands with 3phw.

Connection of docked potent compound 39 at the active site of 3phw produced using the Discovery Studio and LigPlot+ program (Fig. 4), interaction analysis of this complex showed 2 hydrogen bonds and hydrophobic

interactions between compound 39 and the binding site residues of 3phw as well as with some neighboring amino group that can be seen in Figure 5. 3phw residues involved in H-bond formation included Arg9 (3.00 and 3.07Å). Amino acids, Val82, Glu98, Tyr42, Gly100, Ser101, Met93, Glu104, Tyr89, Leu81 and Leu84, Asn97, and Gly83 were making hydrophobic contacts. Binding of the ligand at this site would lead to blocking of ligand-protein interactions between compound 39 and PDB: 3phw.

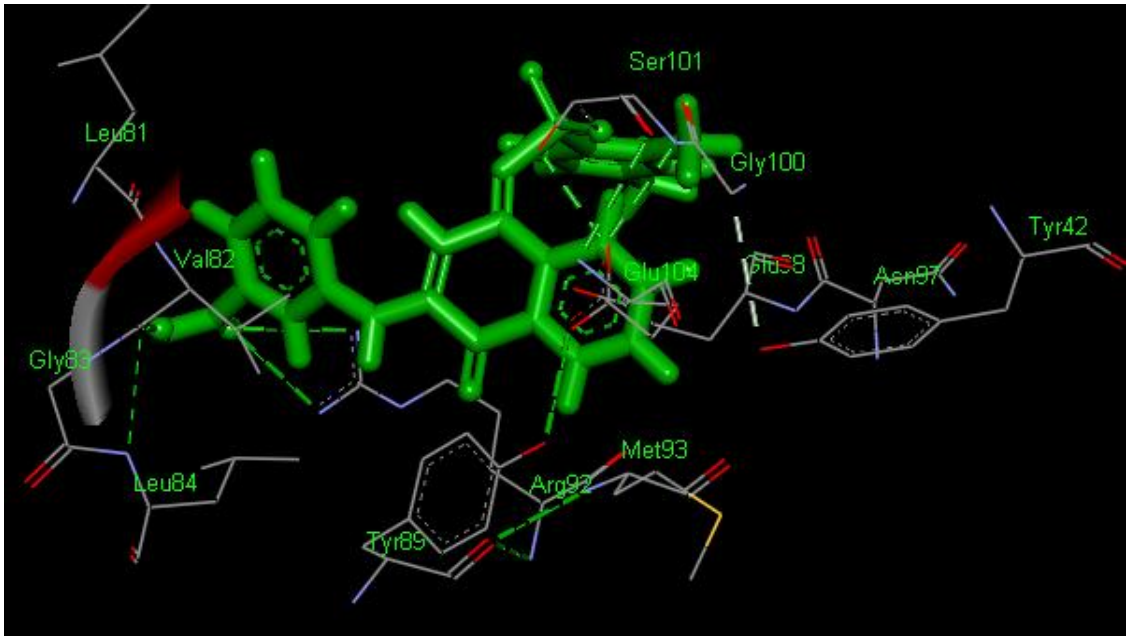

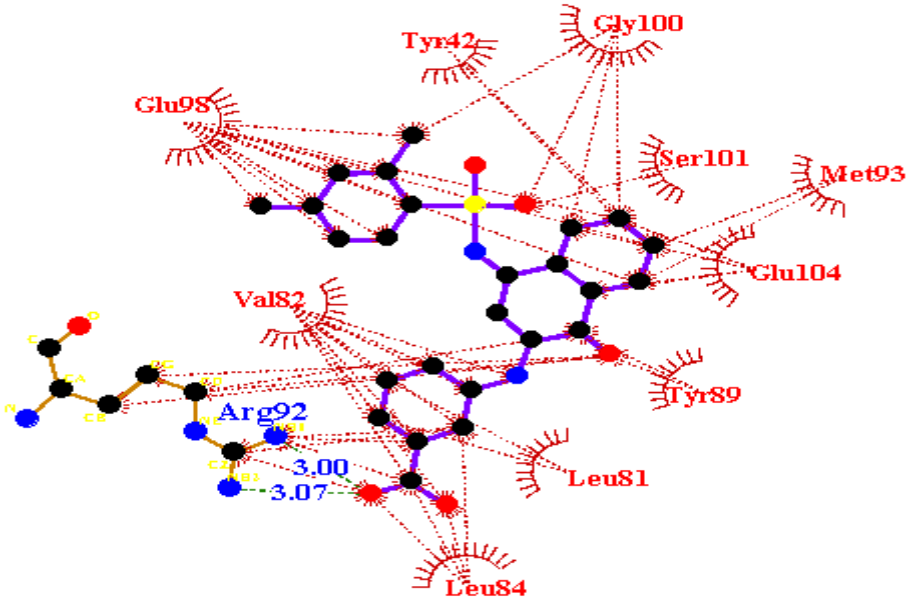

Figure 4: Intersection of docked potent compound 39 at the active site of 3phw produced using the MVD, Discovery Studio and LigPlot+ program

2.3. Protein-Ligand Interaction using PyRx (Autodockvina)

The structures were docked using Autodock vina [21] in the active site defined through a grid box (x = 50.4184757423, y = 41.247352066, z = 33.6435040188), center (x = 4.4456 y = -44.9073, z = -13.8825) and exhaustiveness = 8. The highest docking scores targets, 20 and 39, were found to be −7.7 kcal/mol and −8.2 kcal/mol, respectively. Compound 39 was found interacting with active site residues (Asp32, Gln73, Asp228, Gly230, Thr232, Asn233, and Arg235) of 3phw with the formation of three hydrogen bonds and 7 hydrophobic contacts. Among the residues lining the binding site, Ile157 (2.98 Å) and Asn143 (2.94 Å) were found participating in hydrogen bond formation with the ligand. The other residue participating in H bond formation was Arg5 (3.11Å and 3.13 Å). The residues Val138 of the binding cleft along with numerous neighboring amino acids, namely, Glu162, Arg156, Leu48, Leu155, Ala141, Thr140, and Phe139, were observed to be involved in hydrophobic interactions with ligand 39. The involvement of binding site residues of 3phw with ligand39 would block the OTU Domain of Crimean Congo Hemorrhagic Fever Virus in complex with Ubiquitin interaction, thereby preventing the processing of Crimean-Congo hemorrhagic fever (CCHF) formation. The binding mode of interactions can be well understood through the pictorial representation as shown in Figure 5.

Table 3: Compounds Pubchem_CID number and their Docking Scores

Compound number	Pubchem_CID	Docking Score (Kcal/mol)	PIC_{50}
7	2044030	-7.6	5.119
19	2133777	-7.3	5.666
20	5998602	-7.7	5.987
35	5824722	-6.9	5.701
37	5824727	-7.5	5.601
39	5824726	-8.2	5.627
41	664517	-7.4	5.284
62	392758	-6.5	5.363

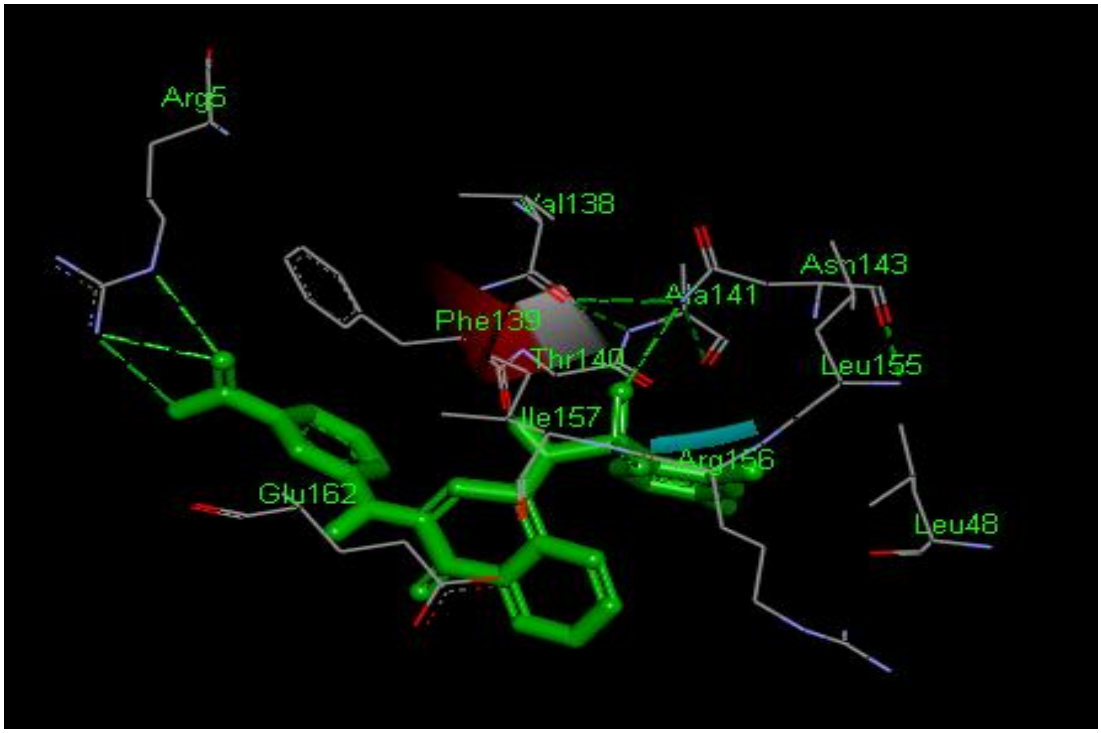

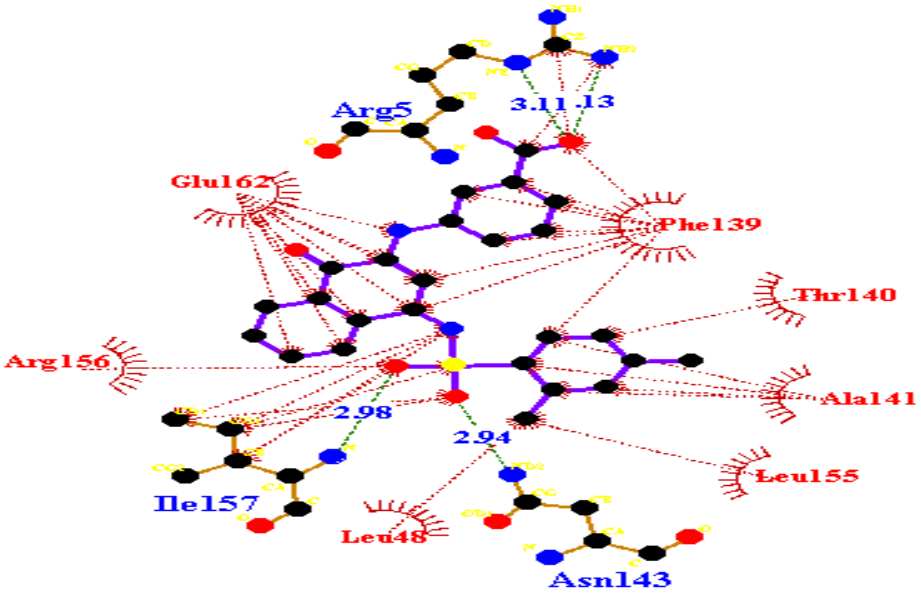

Figure 5: Intersection of docked potent compound 39 at the active site of 3PHW produced using the PyRx, Discovery Studio and LigPlot+ program

Compound 20, interaction analysis of this complex showed 1 hydrogen bond and 12 hydrophobic interactions between the binding site residues of 3phw as well as with some neighboring amino group that can be seen in Figure 6. 3phw residues involved in H-bond formation included Ser101 (2.69Å). Amino acids, Ile118, His146, Leu81, Val82, Arg92, Leu103, Met93, Tyr89, Glu104, Phe152, Thr102, and Gly100, were making hydrophobic contacts. Binding of the ligand at this site would lead to blocking of ligand-protein interactions between ligand 20 and PDB: 3phw.

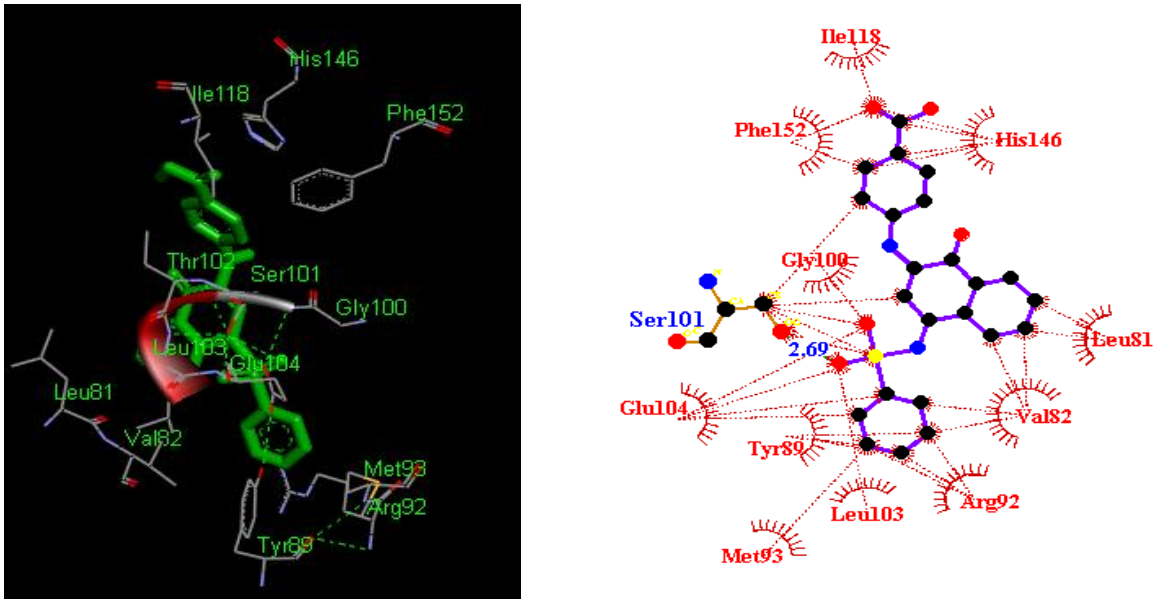

Figure 6: Overlay of docked potent compound 20 at the active site of 3PHW produced using the PyRx, Discovery Studio and LigPlot+ program

The result of MD simulations proved the stability of the protein-ligand complex and provided additional information about the binding mode of compound 39. The root mean square deviation (RMSD) plot and total energy plot of the

complex during the MD simulations are shown in Figure 7. The simulation result reveals that the RMSD tends to be stable and fluctuated around 4.6 Å and the total energy is fluctuated around -24,000 kcal/mol after running 5000;# 100ps, which implies that the structure of the complex is basically in a stable state.Result of molecular dynamics simulations during;minimize 500;# lower potential energy for 1000 step; #reinitvel $temperature;# since minimization zeros velocities; run 5000 ;# 100ps. NVT; RMSD, Bond, Elect, VDM, Kinetic, Total energy, temperature, and Pressavg plot of the protein-ligand complex (Fig. 7).

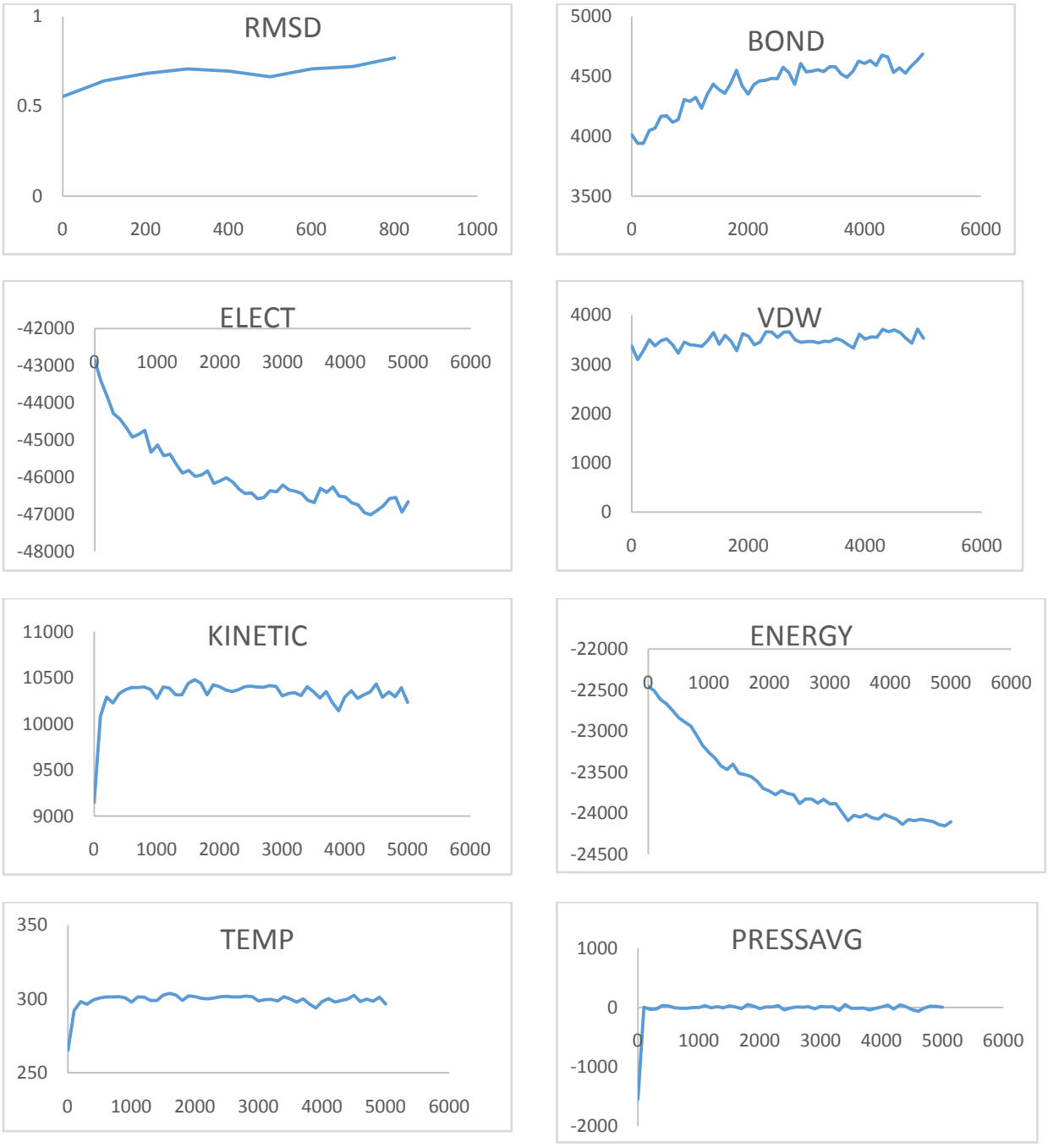

Figure 7: Result of molecular dynamics simulations during.run 5000;# 100ps NVT, RMSD, BOND, ELECT, VDM, Kinetic, TOTAL ENERGY, TEMP., and PRESSAVG plot of the protein-ligand complex

We compared the conformation of the complex after simulation with the initial. The compound 39 adopt a similar pose and was placed in the same region of two structures, which means that the compound can be stably located in the docking site. And then, we compared the residues which interact with compound 39 after the simulation. As shown in Figure 8, compound 39 went deeper into the enzyme binding pocket and this would significantly increase the binding affinity.

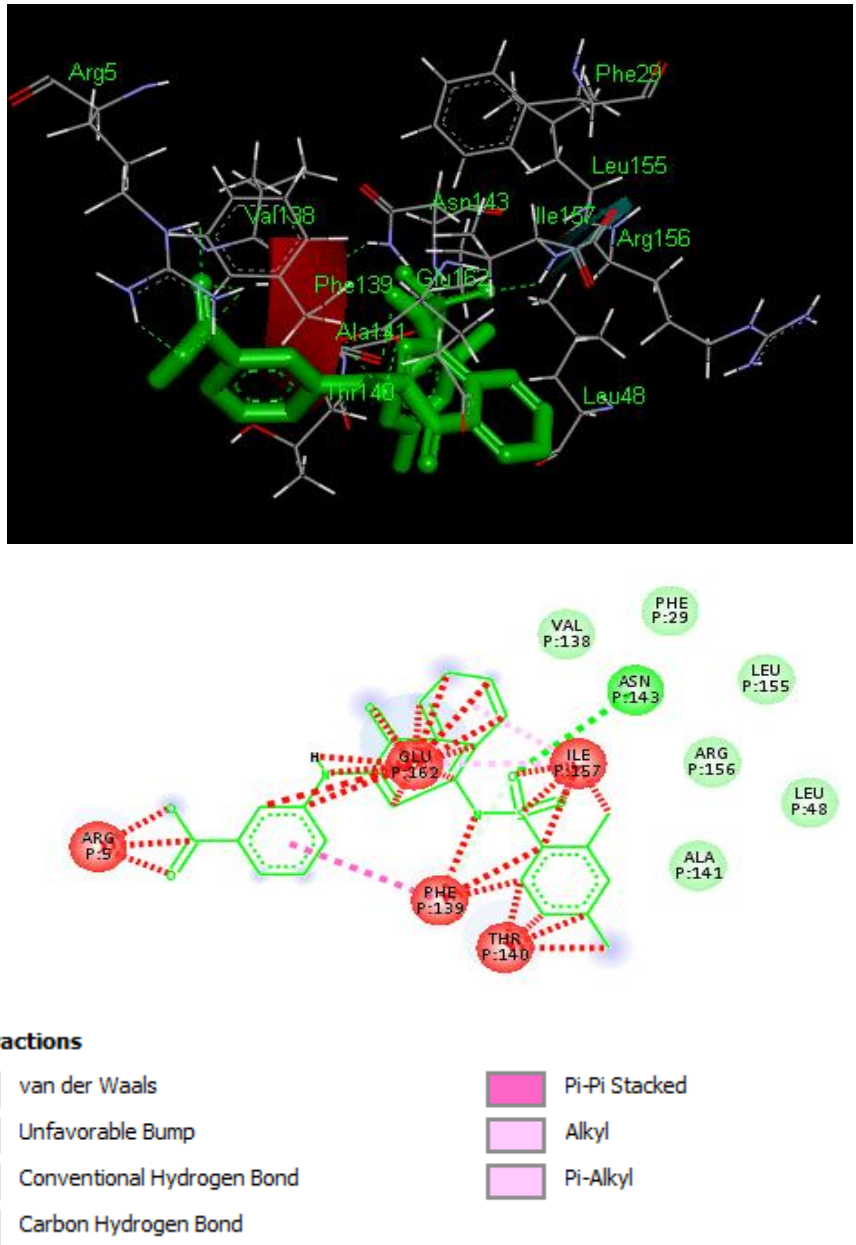

Figure 8: Comparing the protein (PDB code: 3phw) confirmation before and after the simulation

ADME properties, their prediction and lipophilic efficiency calculation (LipE)

The point of comparison between drugs appears to be a desirable reference model for coding the balance between the molecular properties of a compound that influences its pharmacodynamics and pharmacokinetics in the final

analysis, optimizes their absorption, distribution, metabolism, and excretion (ADME) in the human body like a drug [22]. These parameters allow identifying the oral absorption or membrane permeability that occurs when the considered molecule meets the Lipinski's "rule of five" [23, 24] and the rules of Veber and his coworker [25] where they molecular weight (MW) should be ≤500, an octanol-water partition coefficient log P should be ≤ 5, H-bond donors, nitrogen or oxygen atoms with one or more hydrogen atoms (HBD) should be ≤5 and H-bond acceptors, nitrogen or oxygen atoms (HBA) should be ≤10. The total number of violations in this ROF-score, which lies between 0 and 4, shows that good absorption or permeation is more likely to occur. The results obtained are shown in Table 4.

Table 4: Physico-chemical parameters using PowerMV calculation [26]

	XLogP	PSA	NumHBA	NumHBD	MW	BBB	NumRot
19	3.248	141.65	4	2	398.469	0	5
20	4.294	121.28	7	2	432.457	0	5
35	4.731	121.28	7	2	446.484	0	5
37	5.195	121.28	7	2	460.511	0	6
39	5.168	121.28	7	2	460.511	0	5
41	3.656	70.83	5	0	424.456	0	3
62	2.032	29.95	4	1	394.498	1	3
7	6.011	85.26	3	1	448.935	0	5

Table 5: Pharmacological activities and propertiesusing Spartan calculation

Ligand	LogP	HBD	HBA	LE	LipE	LELP
19	-	2	9	-	-	-
20	2.95	2	7	0.2704	3.037	10.91
35	3.44	2	7	0.2494	2.261	13.79
37	3.86	2	7	0.2376	1.741	16.25
39	3.93	2	7	0.2387	1.697	16.46
41	-	0	6	-	-	-
62	-	1	4	-	-	-
7	6.41	1	7	0.2311	-1.291	27.74

LogP is used to predict the solubility of oral drugs. If LogP increases, solubility in water decreases so absorption decreases. A negative value for LogP indicates that the ligand is too hydrophilic. So it has good aqueous-solubility, better gastric tolerance, and efficient elimination through the kidneys. On the other hand, a positive value for LogP indicates that the compound is too lipophilic. So it has a good permeability through the biological membrane, a better binding to plasma proteins, elimination by metabolism but poor solubility and gastric tolerance [27]. In our case, all the values of LogP are positive, so they have a good permeability through a biological membrane. Ligand or compound 20 and 39 have a good value of LogP. Many rotatable bonds (NumRot) is a simple topological parameter that measures molecular flexibility and is considered to be a good descriptor of oral bioavailability of drugs. Rotatable bond is well-defined as any single non-ring bond, bounded to non-terminal heavy (i.e., non-hydrogen) atom. The small number of rotatable bonds in the studied series indicates that these Ligands upon binding to a protein change their conformation only slightly. Rotatable bonds are under 10 so all the screened compounds were flexible, particularly, compound 37 which have 6 rotatable bonds [25]. Total polar surface area (TPSA) is a very useful parameter for the prediction of drug transport properties. Polar surface area is defined as a sum of surfaces of polar atoms (usually oxygen's, nitrogen's, and attached hydrogens) in a molecule. This parameter has been shown to correlate very well with the human intestinal absorption, Caco-2 monolayer's permeability, and blood-brain barrier penetration [28]. Veber rules suggest that molecular flexibility and polar surface area (PSA) are important determinants of oral bioavailability [25]. Molecules with PSA values of 140 A2 or more are expected to exhibit poor intestinal absorption [27]. All compounds chosen have PSA below 140 A2, except compound 19 have PSA above 140 A2.

The molecular weight of all the compound is less than 500. The smaller MW is, the better the absorption will be. All the compounds have MW under 500, therefore, they can easily pass through the cell membrane, blood-brain (BBB) indicator (0 does not go into the brain, 1, goes into the brain) that is, compound 2 goes into the brain. Compounds 20 and 39 have 2 H-bond donors. If there is a small number of hydrogen bond donors, the fat solubility will be high and therefore the drug will be able to penetrate the cell membrane to reach the inside of the cell. The calculation results show that all compounds meet the Lipinski rules [23, 24], suggesting that these compounds theoretically would not have problems with oral bioavailability, since, compounds 20 and 39 were found obey the Lipinski rule and scored the highest docking results, suggested that these compounds theoretically would have no problems with oral bioavailability.

Ligand efficiency (LE) and Lipophilicity efficiency (LipE) are defined as follows:

$$LE = \frac{1.4\ X\ pIC_{50}}{N_H}$$

The lipophilicity is the major factor for the casual and indiscriminate of compounds, LipE optimized compounds should be more selective. It is suggested to target a LipE in a range of 5–7 or even higher [28, 29]. If LipE is between 1 and 3 or over 5, the optimized compounds are more selective.

$$LipE = pIC_{50} - LogP$$

The compounds have LipE more than 1, this indicates that all compounds weresuccessfully optimized, except compound 7. Also, we can see that compound 20 had the highest LipE values of the data was believed to be the most optimal compound. Ligand efficiency-dependent lipophilicity index (LELP) to combine molecular size and lipophilia into a single measure of efficacy. The optimal LELP scores as -10 < LELP < 10 [30].

$$LELP = \frac{LogP}{LE}$$

All the compounds are not located in the suggested range –10 < LELP < 10. Compounds 20, 35, 37 and 39 have their LELP less than 16.50, which means that these compounds are in the Lipinski zone (ROF-score = 4). Except the compound 7 with LELP 27.74 in agreement with its weak ROF-score < 4.

Conclusions

A series of differently substituted compounds have been considered to check their potential biological activity. It has been found that these compounds should exhibit good cell plasma membrane permeability. Furthermore, to identify compounds that have high potency were assayed. The use of Lipinski, Veber, and lipophilicity indices approaches (Table 4 and 5) showed that the compounds 10,12,14,16 have a better BBB permeation, good intestinal permeability, and oral bioavailability, they have a desired in vitro ADME and safety attributes. Compound 19 (Table 4) drugs also meet these rules, so these compounds (20, 35, 37, and 39) are likely to achieve an outcome in the clinic. These results help us to design a successful Crimean-Congo hemorrhagic fever drug, with better anti-Crimean-Congo hemorrhagic fever activity.

Conflict of interest

The authors declare that there is no conflict of interest regarding the publication of this paper. Also, they declare that this paper or part of it has not been published elsewhere.

Acknowledgments

The authors gratefully acknowledge the Department of Chemistry, Ahmadu Bello University, Zaria (Samaru, Zaria-Nigeria); for computational studies, and as part of the Ph.D. thesis.

References

[1]. WHO Media Centre, 2001. Crimean-Congo haemorrhagic fever.

[2]. Welch SR, Ritter JM, McElroy AK, Harmon JR, Coleman-McCray JD, et al. (2019) Fluorescent Crimean-Congo hemorrhagic fever virus illuminates tissue tropism patterns and identifies early mononuclear phagocytic cell targets in IFNAR-/- mice. PLoSPathog 15(12): e1008183. https://doi.org/10.1371/journal.ppat.1008183.

[3]. Scholte FEM, Spengler JR, Welch SR, Harmon JR, Coleman-McCray JD, et al. (2019) Single-dose replicon particle vaccine provides complete protection against Crimean-Congo hemorrhagic fever virus in mice, Emerging Microbes & Infections, 8:1, 575-578. DOI: 10.1080/22221751.2019.1601030.

[4]. Dzimianski JV, Beldon BS, Daczkowski CM, Goodwin OY, Scholte FEM, et al. (2019) Probing the impact of nairovirus genomic diversity on viral ovarian tumor domain protease (vOTU) structure and deubiquitinase activity. PLoSPathog 15(1): e1007515. https://doi.org/10.1371/journal.ppat.1007515.

[5]. Estrada-Pena A, de la Fuente J. (2014) The ecology of ticks and epidemiology of tick-borne viral diseases. Antiviral Res 108C:104–128.

[6]. Capodagli GC, McKercher MA, Bakerm EA, Masters EM, Brunzelle JS, et al. (2011) Structural analysis of a viral ovarian tumor domain protease from the Crimean-Congo hemorrhagic fever virus in complex with covalently bonded ubiquitin. J Virol 85:3621–3630.

[7]. Weber F, Mirazimi A. (2008) Interferon and cytokine responses to Crimean Congo hemorrhagic fever virus; an emerging and neglected viral zonoosis. Cytokine Growth Factor Rev, 19(5-6): p. 395-404.

[8]. Yadav PD, Vincent MJ, Khristova M, Kale C, StNichol ST, et al. (2011) "Genomic analysis reveals Nairobi sheep disease virus to be highly diverse and present in both Africa, and in India in the form of the Ganjam virus variant,"Infection Genetics and Evolution Volume 11, Issue 5, July 2011, Pages 1111-1120. 10.1016/j.meegid.2011.04.001.

[9]. Akutsu M, Ye Y, Virdee S, Chin JW, Komander D.(2011) Molecular basis for ubiquitin and ISG15 crossreactivity in viral ovarian tumor domains. Proc Natl AcadSci USA 108:2228–2233.

[10]. James TW, Frias-Staheli N, Bacik JP, Macleod JML, Khajehpour M, et al. (2011) Structural basis for the removal of ubiquitin and interferon-stimulated gene 15 by a viral ovarian tumor domain-containing protease. Proc Natl AcadSci USA 108:2222–2227.

[11]. Scholte FEM, Zivcec M, Dzimianski JV, Deaton MK, Spengler JR, et al. (2017) Crimean-Congo Hemorrhagic Fever Virus Suppresses Innate Immune Responses via a Ubiquitin and ISG15 Specific Protease. Cell Reports 20, 2396–2407. http://dx.doi.org/10.1016/j.celrep.2017.08.040.

[12]. Ha BH, Kim EE. (2008) Structures of proteases for ubiqutin and ubiquitin-like modifiers. BMB Rep. 41(6), 435-43.

[13]. Frias-Staheli N, Giannakopoulos NV, Kikkert M, Taylor SL, Bridgen A, et al. (2007) Ovarian tumor domaincontaining viral proteases evade ubiquitin- and ISG15-dependent innate immune responses. Cell Host Microbe 2:404–416.

[14]. Chaube U, Chhatbar D, Bhatt H. (2016) 3D-QSAR, molecular dynamics simulations and molecular docking studies of benzoxazepine moiety as mTOR inhibitor for the treatment of lung cancer. Bioorganic & Medicinal Chemistry Letters 26, 864–874.

[15]. Fiolhais C, Nogueira F, Marques M. (2003) A Primer of Density Functional Theory, Springer-Verlag, Berlin, Heidelberg, New York, pp. 218–256.

[16]. Becke AD. (1993) Density-functional thermochemistry 3. The role of exact exchange. J. Chem. Phys.98: 5648.

[17]. Lee C, Yang W, Parr RG. (1988) Development of the Colle-Salvetti correlation-energy formula into a functional of the electron density. Phys Rev. 37, 785–789.

[18]. Akutsu M, Ye Y, Virdee S, Komander D. (2014). OTU Domain of Crimean Congo Hemorrhagic Fever Virus in complex with Ubiquitin. 10.2210/pdb3phw/pdb http://dx.doi.org/10.2210/pdb3phw/pdb.

[19]. Thomsen R, Christensen MH. (2006) MolDock: a new technique for high-accuracy molecular docking. Journal of medicinal chemistry 49, 3315–3321. DOI: 10.1021/jm051197e.

[20]. Phillips JC, Braun R, Wang W, Gumbart J, Tajkhorshid E, et al. (2005) Scalable Molecular Dynamics with NAMD. J Comput Chem. 26(16): 1781-1802.

[21]. Trott O, Olson AJ. (2010) AutoDockVina: improving the speed and accuracy of docking with a new scoring function, efficient optimization and multithreading, J Comp Chem. 31, 455-461.

[22]. Vistoli G, Pedretti A, Testa B. (2008) Assessing drug-likeness - What are we missing? Drug. Discov Today. 13, 285–294.

[23]. Lipinski CA, Lombardo F, Dominy BW, Feeney PJ. (1997) Experimental and computational approaches to estimate solubility and permeability in drug discovery and development settings. Adv. Drug Delivery Rev. 23, 4-25.

[24]. Lipinski C A. (2000) Drug-like properties and the causes of poor solubility and poor permeability. J. Pharmacol. Toxicol. Methods. 44, 235-249.

[25]. Veber DF, Johnson SR, Cheng HY, Smith BR, Ward KW, et al. (2002) Molecular properties that influence the oral bioavailability of drug candidates. J. Med. Chem. 45, 2615–2623.

[26]. Liu K, Feng J, Young SS. (2005) PowerMV: A Software Environment for Molecular Viewing, Descriptor Generation, Data Analysis and Hit Evaluation J. Chem. Inf. Model. 2005, 45, 515-522.

[27]. Rouane A, Tchouar N, Kerassa A, Belaidi S, Cinar M. (2017) Structure-Based Virtual Screening and Drug-Like of Quercetin Derivatives with Anti-Malaria Activity. Reviews in Theoretical Science 5, 1–11. doi:10.1166/rits.2017.1090.

[28]. Wager TT, Chandrasekaran RY, Hou X, Troutman MD, Verhoest PR, et al. (2010) Defining desirable central nervous system drug space through the alignment of molecular properties, in vitro ADME, and safety attributes. ACS Chem. Neurosci. 1, 420–434.

[29]. Pajouhesh H, Lenz GR. (2005) Medicinal chemical properties of successful central nervous system drugs. Neuro Rx. 2, 541–553.

[30]. Keserü GM, Makara GM.(2009)The influence of lead discovery strategies on the properties of drug candidates. Nat. Rev. Drug Discov. 8, 203–212.